

Transformation of head-direction signal into spatial code

Adrien Peyrache^{1,3}, Lisa Roux¹, Natalie Schieferstein¹, Gyorgy Buzsaki^{1,2}

¹ The Neuroscience Institute, ² Center for Neuroscience, New York University Langone Medical Center, New York City, New York, USA

³ Department of Neurology and Neurosurgery, Montreal Neurological Institute, McGill University, Montreal, Quebec, Canada

Abstract

Head direction (HD), boundary vector, grid and place cells in the entorhinal-hippocampal system form the brain's navigational system that allows to identify the animal's current location and to move towards desired goal locations. How the functions of these specialized neuron types are acquired and how their computations relate to each other remain to be understood. We examined how head direction and place information are represented in thalamic, post-subiculum and hippocampal neurons and how their firing patterns are influenced by the ambulatory constraints imposed upon the animal by the boundaries of the explored environment. We show that in the antero-dorsal thalamic nucleus, the HD signal can represent a spurious spatial code under behavioral constraints. In the post-subiculum, the main cortical stage of HD signal processing, the amount of spatial information conveyed by HD neurons is increased by the combination of the HD signal with other sensory modalities. We also demonstrate HD signals in the hippocampus and hypothesize that HD can contribute to the generation of a spatial code. These findings demonstrate how sensory information can be transduced into a spatial code.

Introduction

Sensory signals are processed by the central nervous system in a hierarchical manner (Felleman and Van Essen, 1991). As one moves from the periphery to the core of the brain, the controlling role of sensory inputs on neuronal firing patterns decreases, whereas higher-level features, including multimodal information and accumulated memory, play an increasing role (Pastalkova et al., 2008). Striking examples of such transformation are the integration of sensory features into spatial information by the grid cells in the entorhinal cortex (Hafting et al., 2005; McNaughton et al., 2006) and place cells in the hippocampus (O'Keefe and Dostrovsky, 1971; O'Keefe and Nadel, 1978). Together, they form the basis of a cognitive map (O'Keefe and Nadel, 1978) and convey the highest amount of spatial information in the limbic system (Hargreaves et al., 2005; Wilson and McNaughton, 1993). Yet, it is not well understood how spatial information arises from sensory inputs (O'Keefe and Burgess, 1996).

The head direction system (Ranck, 1985; Sharp et al., 2001; Taube, 1995, 2007; Taube et al., 1990a) is a critical part of the navigation system (McNaughton et al., 2006; Winter et al., 2015). The head-direction signal originates in the vestibular system (Sharp et al., 2001; Taube, 1995, 2007) and is updated by external sensory inputs, including visual information (Acharya et al., 2016; Clark et al., 2012; Taube et al., 1990b; Zugaro et al., 2003) that references the signal to the environment. The HD signal thus constitutes the simplest allocentric signal of the navigation system. It is conveyed to the parahippocampal region by the antero-dorsal nucleus of the thalamus (ADn) (Sharp et al., 2001; Taube, 2007). The post-subiculum (PoS) is the main cortical recipient of ADn output (Ding, 2013; Peyrache et al., 2015; Shibata, 1993) and acts as a relay of HD signal to the other structures of the parahippocampal system (Ding, 2013; Preston-

Ferrer et al., 2016; Tukker et al., 2015). In addition, the PoS receives inputs from different sensory and association cortices (Ding, 2013) and, thus, occupies a central position in the chain of spatial information processing. In turn, the feedback arising from the PoS onto thalamic HD neurons updates the HD representation and aligns it to the external world (Goodridge and Taube, 1997). The HD signal, conveyed directly (Shibata, 1993) or indirectly (Ding, 2013; Preston-Ferrer et al., 2016; Tukker et al., 2015) by ADn neurons, is present in all structures of the parahippocampal circuit (Acharya et al., 2016; Chen et al., 1994; Leutgeb et al., 2000; Rubin et al., 2014; Sargolini et al., 2006; Tang et al., 2016; Taube et al., 1990a).

Using various empirical metrics and, often, arbitrary threshold criteria, a variety of neuron classes have been segregated and named (Boccaro et al., 2010; Brandon et al., 2011; Cacucci et al., 2004; Giocomo et al., 2014; Hinman et al., 2016; Kropff et al., 2015; Lever et al., 2009; Sargolini et al., 2006; Savelli et al., 2008; Sharp, 1996; Solstad et al., 2008; Tang et al., 2016), although the boundaries among these classes are not uncontested (Krupic et al., 2012).

Whereas place cells in the hippocampus and grid cells in the entorhinal cortex are undisputed classes of the brain's navigation system, most neurons in the parahippocampal regions represent intermediate forms. Many neurons unite two or more features (referred to as conjunctive cells) (Sharp, 1996), for example conjunctive grid cells with both spatial and HD information (Boccaro et al., 2010; Brandon et al., 2011; Sargolini et al., 2006). Border cells or boundary vector cells observed within the medial entorhinal cortex and other parahippocampal structures, fire preferentially at the edges of the environment or signal the distance from the animal to the borders (Lever et al., 2009; Savelli et al., 2008; Solstad et al., 2008). Border and HD neurons emerge at the earliest stage of ontogenetic development and precede the development of grid cells and place cells (Bjerknes et al., 2014, 2015; Langston et al., 2010; Tan et al., 2015; Wills et al., 2010). HD neurons and border cells, therefore, may be considered as fundamental building blocks of the spatial code (O'Keefe and Burgess, 1996). In support of this hypothesis, grid representation is severely impaired after destruction of ADn neurons

(Winter et al., 2015). Furthermore, the geometry of the environment exerts a strong influence on the development and firing patterns of place and grid fields (Krupic et al., 2015; O'Keefe and Burgess, 1996; Stensola et al., 2015).

Despite all these important results, it remains to be demonstrated how activity of HD neurons, sensory information and active exploration by the animal interact and assist in the emergence of a spatial map. In the present experiments, we demonstrate how the animal's behavior itself can influence spatial metric (Wiltschko et al., 2015). Specifically, we present evidence that, because of stereotypical behaviors, HD cells in the thalamus (ADn) convey spatial information from the viewpoint of a downstream reader. In contrast, HD cells in the PoS convey true spatial information by combining the allocentric HD information with body-centered, egocentric signals, such as the relationship between the ambulatory pattern of the mouse and boundaries of the environment. Such conjunction may be the first stage of computation that integrates primary information to establish the cognitive map.

Results

Neurons were recorded in the anterior thalamus, the post-subiculum and the CA1 subfield of the hippocampus of freely moving mice. In ADn neurons, HD information was high and uniform with a narrow unimodal distribution (see METHODS), demonstrating that neurons of this thalamic nucleus selectively carry HD signal. In contrast, PoS and CA1 units represent a mixture of neurons from high to low values of HD information. While spatial information was highest in CA1 with little overlap between HD and place-specific neurons, it was comparably high in ADn and PoS pyramidal cells, implying that HD neurons may also carry spatial information.

It is often assumed that the role of the HD signal is to update, in combination with speed and other proprioceptive information, the current estimate of the position by path integration (Burgess et al., 2007; Etienne and Jeffery, 2004; McNaughton et al., 2006; Mittelstaedt and Mittelstaedt, 1980; Samsonovich and McNaughton, 1997). However, our results show that HD neurons convey a significant amount of spatial information (Figure 1A). The HD information to parahippocampal and hippocampal structures may be conveyed in a serial manner. Alternatively, the place coding system could gain direct HD input from ADn, representing a distributed organization (Figure 1B).

By definition, a ‘pure’ head direction signal is affected by the HD of the animal and nothing else. On the other hand, the spatial specificity of spiking of HD neurons is inevitably affected by the presence of environmental boundaries (Cacucci et al., 2004). Since not all head directions can be displayed equally near the walls, this bias results in a non-uniform distribution of spikes, as illustrated for an example ADn HD neuron (Figure 2A). The neuron exhibits strikingly higher firing rates along the walls parallel to the preferred orientation. As a result of such physical constraint, the amount of *spatial* information conveyed by this cell (~0.6 bit/spike) is comparable in magnitude to information reported in other parahippocampal areas and cell types (Hargreaves et al., 2005; Wills et al., 2010). However, this spatial information is spurious, and can be attributed to the wall-constrained non-uniform distribution of spikes (Cacucci et al., 2004). To estimate the neuron’s true spatial information, independent of its HD tuning, we generated series of random spike trains drawn from a Poisson distribution depending exclusively on the current heading of the animal at each point in time and the cell’s HD tuning curve. We therefore defined the ‘unbiased spatial information’ conveyed by a neuron, as the difference between the observed and control (i.e., HD-corrected) information per spike. An example of such a spike train displays a very similar non-uniform spatial distribution (Figure 2B), resulting in equally high level of spatial information. The low unbiased spatial information of this

HD neuron shows that the neuron was only modulated by the head-direction of the animal (for further examples, see Figure 2C-D and S1).

Figure 2E illustrates how the HD probability distribution is affected by the presence of the walls. North (“N”) and South (“S”) orientations occurred more frequently along the East (“E”) and West (“W”) walls because mice rarely run straight all the way to the walls. Instead, they turn and run parallel with the wall. Similarly, E and W orientations concentrated more frequently along the N and S walls. The animal’s orientation bias was measured as the concentration of the animal’s heading in the two possible directions parallel to the walls. Concentration was significantly higher 10 cm or less from the nearest walls than at the center of environment, measured between 15-25 cm from the walls ($p < 10^{-7}$, Mann-Whitney U test; Figure 1D). These findings demonstrate that animals exhibit biased behavior while exploring an open environment with boundaries.

Next, we quantified the relationship between HD and spatial information, using the above methods, for all recorded neurons in the thalamus and PoS. When restricted to neurons with HD information (see METHODS), spatial and HD information rates were positively correlated in both ADn (black dots in Figure 3A, b; $r = 0.59$, $n=205$, $p < 10^{-10}$, Pearson’s test) and PoS ($r = 0.81$, $n=88$, $p < 10^{-10}$, Pearson’s test). This correlation did not depend on other factors, such as firing rate difference between neurons (partial correlations with firing rates accounted for less than 5% of the HD-spatial information correlation). The correlation between HD and spatial information showed a maximum for a spatial binning of 4-6cm (Figure 3B), although spatial information monotonically decreased with spatial binning (Figure S2A). The same relationship was observed between HD and spatial information when spatial information was estimated with a cross-validated procedure (Figure S2B-E).

Putative pyramidal neurons in the PoS that were not classified as HD neurons still conveyed significant amount of HD information and spatial information, compared for example with putative interneurons (Figure 3C). When spatial information was corrected for the animal's behavior through the procedure described above (see Figure 2A-B), the resulting actual spatial information vanished in ADn neurons but persisted in PoS HD neurons, as well as other putative excitatory cells (Figure 3D, red dots in Figure 3A). Hence, PoS neurons convey actual spatial information. The remaining unbiased spatial information was comparable between PoS HD cells and non-HD pyramidal cells ($p=0.2$, Mann-Whitney U test).

The positive correlation between HD and spatial information was present not only in the open field but even more so in a multi-arm maze (Figure 4A-C, $p<10^{-10}$ for both conditions, $n=57$ ADn neurons, Pearson's test) where the mouse behavior is even more constrained. As a result, the 'gain' (slope of spatial versus HD information) was stronger in the radial arm maze than in the open field ($p=7.7 \cdot 10^{-5}$, t-test) although the HD information was similar in both conditions (Figure 4D; $p>0.05$, sign test).

How do PoS neurons convey actual spatial information? The PoS neurons, in addition to thalamic afferents, also receive inputs from sensory cortices (Ding, 2013). In contrast to ADn neurons, the example HD cell from the PoS (Figure 5A-C) fired mainly along E wall, parallel with its HD tuning curve but less so along the W wall. It conveyed more than 1 bit of spatial information per spike and approximately half of this information could not be explained by its HD tuning curve and behavioral bias alone (Figure 5C). We hypothesized that this neuron integrated the HD signal with specific sensory information, hence HD information was biased by behavioral and environmental features. We tested this hypothesis with a Generalized Linear Model (Harris, 2005; Truccolo et al., 2005) by regressing the HD information separately against each one of the 4 walls. The example neuron was positively modulated by the presence of the

animal along the E wall (Figure 5D). This extra sensory modulation may reflect input from a spatially localized cue (E wall) or could reflect an 'egocentric' signal: "a wall is on my left side". To differentiate between these possibilities, we also regressed the example neuron's firing pattern with a signal informing whether a wall was situated on the right or left side of its body. This analysis revealed that the firing of this neuron was better predicted by the combination of HD and a wall being on the left side of the body (Figure 5D; see Figure 5E-F and Figure S3 for more examples). At the population level, HD and other pyramidal neurons in the PoS (many of which convey significant amount of HD information independent of whether they were classified as HD neurons or not; see Figure 1A) showed significantly stronger modulation by their preferred border than thalamic ADn neurons (Figure 5G; ADn HD neurons vs. PoS HD and non-HD neurons $p < 0.001$; $n = 204, 88, 76$ ADn HD neurons, PoS HD neurons and non-HD neurons respectively; Mann-Whitney U test). Unbiased spatial information was mainly conveyed by principal neurons in the entire cell population in the PoS: as a comparison, the difference between ADn HD neurons and PoS interneurons was significant ($p < 0.01$; $n = 76$ PoS INT; Mann-Whitney U test) but small (0.054 vs. 0.046) and non-significant when a parametric test was used ($p > 0.05$; t-test). In addition, similar differences between ADn and PoS HD neurons were observed when spike trains were regressed against the position of the animal relative to the walls (Figure S4).

Modulation by borders did not differ between areas when cells were regressed only against the presence of the walls (i.e. without the instantaneous expected firing rate from their HD tuning curve): in this case, ADn HD neurons do convey 'spurious' modulation by walls (Figure S4). Overall, the spatial correlates of PoS neurons, independent of whether they conveyed HD information or not, were correlated with their wall-body (Figure 5H; $r = 0.31$, $p < 0.01$; Pearson's test; $p > 0.05$ for ADn HD neurons), suggesting that this additional source of information explains the unbiased information observed in PoS HD neurons.

The subset of neurons with high unbiased spatial information may be additionally driven by non-vestibular sensory inputs or hippocampal output signals. They are thus less likely to exhibit invariant coordination across brain states, especially during sleep when the system is disengaged from its external inputs (Peyrache et al., 2015). To test for this hypothesis, we compared pairwise correlations of HD cells in wake and sleep (either Rapid Eye Movement – REM – or non-REM sleep stages). PoS HD neurons conveying low unbiased spatial info (cell pairs of neurons within the first 33th percentile) had highly preserved correlations during wake and sleep (Figure 6A,B). In contrast, HD cell pairs that were the most spatially tuned (top 33th percentile) had much less wake preserved correlations in both REM and non-REM (Figure 6A,B; Fischer's test, $p < 0.01$ for wake versus REM and non-REM, $n = 35$ and 37 cell pairs in the bottom and top 33th percentile, respectively). ADn HD neurons showed an almost perfectly preserved correlations across brain states (Figure 6B; $p > 0.05$; $n = 164$ and 202 pairs of bottom and top 33th percentile, respectively) in agreement with the hypothesis that neurons of the HD circuits are coordinated by internal dynamics that are largely independent of brain state (Peyrache et al., 2015).

Does the hippocampal network also directly utilize the HD signal from the ADn to generate a place code? This is a possibility as the hippocampus also contains HD neurons (Acharya et al., 2016; Leutgeb et al., 2000; Rubin et al., 2014). These HD cells are often recorded outside the pyramidal layer (Leutgeb et al., 2000) as seen on an example recording from a silicon probe where three HD neurons were isolated on the medio-dorsal portion of CA1 in the alveus/oriens layers (Figure 7A). HD units in the hippocampus were synchronous with HD neurons in the ADn at a submillisecond timescale as shown by the near 0-lag peak in the cross-correlograms between ADn and hippocampal HD neurons with overlapping tuning curves (Figure 7B). The synchronization score (see METHODS) between ADn HD neurons and hippocampal HD neurons was higher than with non-HD neurons ($p < 0.05$; $n = 12,51$ hippocampal HD and non-HD

neurons respectively; Mann Whitney U test). We also found one hippocampal HD neuron that showed a ~5ms delay with ADn spikes, a time lag characteristic of synaptic delay. In the same session, another neuron recorded in the alveus was synchronous with ADn neurons (Figure S5). Finally, hippocampal HD neurons were significantly less entrained by theta oscillations than other hippocampal neurons (a/o HD neurons vs. PYR, $p < 0.001$; vs. r/p INT: $p < 0.01$; vs. a/o INT: $p < 0.01$; $n = 11$ a/o HD neurons, 101 PYR, 21 r/p INT and 21 a/o INT; Mann-Whitney U test), similarly to HD neurons from the ADn (Figure 7D-E).

Discussion

We demonstrate here that HD signals are present at every stage of the spatial navigation signal. HD cells can carry spurious spatial information under environmental constraints. HD neurons in ADn showed symmetric, elongated 'place fields'. The symmetry was broken in PoS neurons by the addition of sensory information so that the place fields meet the criteria of 'border cells' firing most effectively close to one of the walls, demonstrating how sensory information can convert HD signal into a spatial code. The hippocampus was dominated by *bone fide* place cells, with only a minority of neurons expressing HD information. The presence of sharply tuned HD units in the alveus/oriens in the medial CA1 region suggested that thalamic HD information can directly reach each stage of the navigation system in a parallel manner. Our findings demonstrate how the combination of the HD signal and egocentric information leads to a spatial signal.

If the animal's head orientation were unrestricted and homogenous at all locations, the HD system would convey a pure head direction signal, irrespective of the animal's position.

However, most animals live in structured environments and possess genetically determined stereotypical behaviors; for example, rodents are agoraphobic and preferentially walk along borders and sheltered routes (Horev et al., 2007; Wiltschko et al., 2015). When environmental signals are combined with HD signals, the downstream ‘reader’ networks can establish a probabilistic inference about the animal’s position. Since firing of HD neurons is controlled mainly by distal cues (Zugaro et al., 2001), whereas local cues can inform the brain about nearby walls, the combined information can be used to represent environmental boundaries.

The definition of borders is crucial in calibrating a spatial representation (Diba and Buzsaki, 2008; Doeller et al., 2008; Gothard et al., 1996; Krupic et al., 2015; Muller and Kubie, 1987; O’Keefe and Burgess, 1996; Samsonovich and McNaughton, 1997; Stensola et al., 2015). In addition, borders serve as a ‘reset’ signal to correct for accumulated errors of path integration (Etienne et al., 2004; Hardcastle et al., 2015). ‘Border cells’ or ‘boundary vector cells’ in the medial entorhinal cortex and surrounding areas are active along a specific wall of the enclosure (Lever et al., 2009; Savelli et al., 2008; Solstad et al., 2008). The origin of this code remains unknown but border cells are assumed to rely on low-level sensory signals. This may explain why border cells and HD cells emerge early in development, prior to grid cells and place cells, which may require extensive exploration of the environment (Bjerknes et al., 2014, 2015; Langston et al., 2010; Tan et al., 2015; Wills et al., 2010).

Local sensory inputs can be provided by activation of the whiskers (haptic flow) or optic flow near walls. We observed that the association of the HD signal with local egocentric information can break symmetries imposed by the environment (Krupic et al., 2015; Stensola et al., 2015). Active sensing with whiskers can generate a distance code of the nearest wall in the barrel cortex (Sofroniew et al., 2015). As a result of symmetry breaking, spatial information can be incorporated by HD neurons in the PoS (Cacucci et al., 2004). A “pure” HD cell in a square

environment tends to fire along the two opposite walls parallel to its preferred direction.

However, when its HD tuning is combined with an egocentric signal, the cell fires only along one of the walls, effectively doubling its spatial information content (as in the example neuron in Figure 5A-C). The combination of these two streams of inputs, HD and local egocentric, may be considered as building blocks of a code for environment boundaries. When the walls are not parallel to the preferred direction of HD neurons, for example in circular environments, such mechanism may fail (Savelli et al., 2008). These cells can also be influenced by hippocampal outputs or other sensory inputs and may thus combine HD and place signals.

ADn neurons, and member cells of the HD circuit in general, are believed to be endowed with attractor dynamics, emerging from local circuits or inherited from upstream attractors (Knierim and Zhang, 2012; Sharp et al., 2001; Taube, 2007). This hypothesis was confirmed by the demonstration that temporal coordination between HD neurons was strongly preserved across brain states, suggesting a system largely driven by internally generated activity (Peyrache et al., 2015). In contrast, spatially tuned HD neurons that are driven by external signals may reduce their temporal coordination in other behavioral contexts, for example during sleep. In agreement with this hypothesis, the coordination between HD neurons in the PoS that were the most spatially modulated was much less preserved during sleep compared to wake than HD neurons with no or limited spatial modulation. These findings point to the relatively ‘rigid’ and plastic properties of the members of the HD and spatial systems, respectively.

The organization of the HD circuit is often described as a labeled line, bottom-up network where cortical feedback is primarily involved in aligning the signal with the external world (Sharp et al., 2001; Taube, 2007). However, the ADn projects to multiple locations of the parahippocampal formation (Ding, 2013; Shibata, 1993). In addition, our findings indicate that certain HD cells in the PoS may convey more information beyond the HD signal (Cacucci et al., 2004). Similarly,

the MEC is reached directly by ADn neurons (Shibata, 1993), where some neurons exhibit a conjunction of HD and grid signals (Brandon et al., 2011; Sargolini et al., 2006). More generally, neurons in the MEC and the subicular complex exhibit a wide range of combination of spatial, HD and speed signals (Boccaro et al., 2010; Brandon et al., 2011; Cacucci et al., 2004; Giocomo et al., 2014; Hinman et al., 2016; Kropff et al., 2015; Sargolini et al., 2006; Sharp, 1996; Tang et al., 2016). The HD signal present in many neurons of these structures can ultimately support a spatial map or a path integration process.

HD information is essential for maintaining grid cells of the entorhinal grid cells (Winter et al., 2015) and may also be important for hippocampal place cells. Although HD and spatial signals get combined in several structures, the two streams of information appear to keep their identity. Neurons with true spatial properties are modulated by hippocampal theta oscillations (Brandon et al., 2011) and neurons modulated by the theta rhythm provide a dynamical definition of the limbic system (Buzsáki, 2002). In contrast, 'pure' HD neurons, independent of the structure in which they reside, are not affected by theta oscillations (Brandon et al., 2011; Cacucci et al., 2004). Instead, members of the HD system communicate by a fast oscillations (150-250 Hz; (Peyrache et al., 2015). These separate streams may serve to distinguish between externally imposed and internally coordinated mechanisms.

Materials and Methods

Electrodes, surgery and data acquisition.

Some of the data from the present report were previously published (Peyrache, 2015). Briefly, seven mice were implanted with silicon probes (4, 6 or 8 shank, 32 or 64 channel Buzsaki probes, Neuronexus, MI) in the ADn (coordinates from bregma: Antero-Posterior: -0.6 mm; Medio-Lateral: -0.5 to -1.9 mm; Dorso-Ventral: 2.2 mm). Three out of these seven mice were also implanted over the post-subiculum (coordinates from bregma: AP: -4.25 mm; ML: -1 to -2 mm; DV: 0.75 mm). Three mice that were implanted in the ADn but not in the PoS were implanted with five 50 μ m diameter tungsten wires over CA1. Three other animals were implanted over CA1 with one 8 shank, 64 recording site silicon probe (one animal) or two 4 shank, 32 site probes bilaterally (two animals) (coordinates: AP: -1.7; ML: \pm 1.1).

During the recording session, neurophysiological signals were acquired continuously at 20 kHz on a 256-channel Amplipex system (Szeged; 16-bit resolution, analog multiplexing). The wide-band signal was downsampled to 1.25 kHz and used as the LFP signal. For tracking the position of the animals on the open maze and in its home cage during rest epochs, two small light-emitting diodes (5-cm separation), mounted above the headstage, were recorded by a digital video camera at 30 frames per second. The LED locations were detected online and resampled at 39 Hz by the acquisition system. Spike sorting was performed semi-automatically, using KlustaKwik (<http://klustakwik.sourceforge.net/>). This was followed by manual adjustment of the waveform clusters using the software Klusters.

After 4–7 d of recovery, probes were lowered towards their target structures. In animals implanted over the ADn, the thalamic probe was lowered until the first thalamic units could be detected on at least 2–3 shanks. At the same time, hippocampal wires were slowly lowered until

reaching the CA1 pyramidal layer, characterized by high amplitude ripple oscillations. The relative location of the other wires was further assessed by ripple-triggered field potentials (see Figure Supplementary 5). One or two individual neurons could usually be isolated from these wires using same isolation procedure as for high-density silicon probes. The thalamic probe was then lowered by 70–140 μm at the end of each session. In the animals implanted in both the thalamus and in the PoS, the subicular probe was moved everyday once large HD cell ensembles were recorded from the thalamus. Thereafter, the thalamic probes were left at the same position as long as the quality of the recordings remained. They were subsequently adjusted to optimize the yield of HD cells. To prevent statistical bias of neuron sampling, we discarded from analysis sessions separated by less than 3 d during which the thalamic probe was not moved. In animals implanted with silicon probes over CA1, probes were lowered until the CA1 region is reached. Only one session per animal was analyzed in the current manuscript.

Recording sessions and behavioral procedure.

Recording sessions were composed of exploration of an open environment (wake phase) followed and preceded by rest/sleep epochs. Animals implanted in the ADn were foraging for food for 30–45 mins in a 53- × 46-cm rectangular arena surrounded by 21-cm-high, black-painted walls on which were displayed two salient visual cues. A total of 37 sessions showing homogeneous visit within the environment were analyzed. Two of the four only animals implanted in the ADn (not the PoS) explored a radial arm maze (three sessions each) in addition to the open environment (Figure 4). Animals implanted with silicon probes over CA1 explored a circular maze (80 cm in diameter). All experiments were carried out during daylight in normal light-dark cycle.

All behavioral measures were computed when the animal was in movement (speed >2.5 cm/s)

Head-direction neurons. HD tuning curves were obtained by counting the number of spikes for each head direction (in bins of 6°) and then divided by the occupancy (in seconds) of the animal in each direction bin. Neurons were categorized as HD cell when a shuffling of their spike train resulted in a significant resulting vector (1000 shuffles, $p \leq 0.001$), when they showed high stability between the first and second half of the session (Pearson's correlation between the tuning curves $r > 0.75$) and the concentration factor of the spikes' phases around their mean of the tuning curve was higher than 1 (Fisher 1993).

Information measure. Spatial (or HD) information was first computed as the mutual information between animal's location (or HD) and the neurons' firing rate at each location (Skaggs, 1994).

$$I = \sum_x \lambda(x) \log_2 \frac{\lambda(x)}{\lambda} p(x)$$

where x is either a spatial or head-direction bin, $\lambda(x)$ is the firing rate of the neuron in the bin x , λ is the mean firing rate and $p(x)$ is the probability of occupancy at bin x .

Spatial mutual information decreases monotonically with the size of spatial bins. To control for this potential confound, in Supplementary Fig. 3, spatial information was estimated through a cross-validation procedure (Harris 2004). 90% of the data was used to estimate the 'place field' of the neuron (*training* data). This tuning curve was then used to predict the instantaneous firing rate of the neuron during the remaining 10% of the data (*test* data). Spatial binning was fixed (0.5 cm) and place field computed from the training data were smoothed with Gaussian kernels of different spatial variance. Spike trains that showed at least a maximum within the range of spatial smoothing (0.5 - 25 cm) were best predicted with a spatial scale of 2-4 cms.

Unbiased spatial information. 500 control spike trains were generated for each neuron as random Poisson process depending only on the HD tuning curve of the actual neuron and instantaneous heading of the animal. The difference between the observed spatial information and the average spatial information from the random spike trains was defined as the unbiased information. This indicates the amount of spatial information that did not depend on the HD tuning of the neuron.

Behavioral bias. For each position, the histogram of orientation was computed as the histogram of the double values of animal's heading. This doubling transforms direction into orientation, e.g. 90° and 270° are, when doubled, both equal to 180° (modulo 360°). Average orientation values were computed as the direction of the resulting vector. Concentration factor was estimated by assuming the distribution followed a Von Mises' distribution (Fisher, 1993).

Generalized Linear Model. Binned spike trains were regressed with different observables using a logarithmic 'link' function, assuming that spike trains are Poisson processes (Truccolo 2005; Harris, 2004). To estimate the modulation by borders, binned spike trains were regressed on four binary variables indicating the presence of the animals along each of the wall (at less than 15 cms). The four corners were excluded. 'Border modulation' was defined as the maximal regression coefficient among the four coefficients associated with each wall. To estimate how this modulation was independent from spiking directly explained by the HD tuning curve, the neurons were additionally regressed on the instantaneous firing rate expected from the current heading of the animal and the neuron's HD tuning curve.

To estimate the modulation by egocentric signals, binned spike trains were regressed on position of the animal relatively to the walls, defined as two binary values indicating whether the nearest wall (at most 15 cms away) was on the right or left side of the animal ($\pm 60^\circ$). 'Egocentric modulation' was defined as the absolute difference between the regression coefficients

associated with the wall on the right or the left of the animals. Similarly to the modulation by border, binned spike trains were additionally regressed on the instantaneous firing rate drawn from their HD tuning curve (as shown in Fig. 5c).

To normalize the contribution of each variable, they were z-scored. In addition, binned spike trains were regressed on an additional constant term (of constant value). This is equivalent to making the resulting coefficients independent of neurons' firing rates.

Mathematically, this corresponded to determine the vector of unknown parameters β that best explained the firing rate $\lambda_i(t)$ of cell i at time t through the relation:

$$\lambda_i(t) = \exp\left(\beta_{i,0} + \sum_{k=1}^N \beta_{i,k} X_k(t)\right)$$

where $X_k(t)$ is the (z-scored) value of the k th observable (out of N) at time t , the term $\beta_{i,0}$ captures the average activation of the neuron (equivalent to a parameter associated with an observable of constant value) and $\beta_{i,k}$ is the parameter associated with the k th observable for neuron i .

Synchronization score (presented in Figure 6 and S6). Cross-correlograms were convolved with a 10ms s.d. Gaussian window to determine the baseline where sub-millisecond interaction are smoothed out. The interval of confidence was determined by assuming the cross-correlograms are drawn from Poisson distributions, evaluated at $p < 0.01$.

Acknowledgement

The work was supported by US National Institute of Health grants NS34994, MH54671 and NS074015, the Human Frontier Science Program. A.P. was supported by EMBO Fellowship ALTF 1345-2010, Human Frontier Science Program Fellowship LT000160/2011-I and National Institute of Health Award K99 NS086915-01. L.R. was supported by National Institute of Health Award K99 NS094735.

Author Contribution

A.P. and G.B. designed the experiments. A.P. and L.R. conducted the experiments. A.P. designed and performed the analyses with the help of N.S. A.P. and G.B. wrote the paper with input from L.R.

Data accessibility

Data are available at <http://crcns.org/data-sets/thalamus/th-1> (doi:10.6080/K0G15XS1).

Bibliography

Acharya, L., Aghajan, Z.M., Vuong, C., Moore, J.J., and Mehta, M.R. (2016). Causal Influence of Visual Cues on Hippocampal Directional Selectivity. *Cell* 164, 197–207.

Bjerknes, T.L., Moser, E.I., and Moser, M.-B. (2014). Representation of Geometric Borders in the Developing Rat. *Neuron* 82, 71–78.

Bjerknes, T.L., Langston, R.F., Krugé, I.U., Moser, E.I., and Moser, M.-B. (2015). Coherence among head direction cells before eye opening in rat pups. *Curr. Biol.* CB 25, 103–108.

Boccarda, C.N., Sargolini, F., Thoresen, V.H., Solstad, T., Witter, M.P., Moser, E.I., and Moser, M.-B. (2010). Grid cells in pre- and parasubiculum. *Nat. Neurosci.* 13, 987–994.

Brandon, M.P., Bogaard, A.R., Libby, C.P., Connerney, M.A., Gupta, K., and Hasselmo, M.E. (2011). Reduction of Theta Rhythm Dissociates Grid Cell Spatial Periodicity from Directional Tuning. *Science* 332, 595–599.

Burgess, N., Barry, C., and O'Keefe, J. (2007). An oscillatory interference model of grid cell firing. *Hippocampus* 17, 801–812.

Buzsáki, G. (2002). Theta oscillations in the hippocampus. *Neuron* 33, 325–340.

Cacucci, F., Lever, C., Wills, T.J., Burgess, N., and O'Keefe, J. (2004). Theta-modulated place-by-direction cells in the hippocampal formation in the rat. *J. Neurosci. Off. J. Soc. Neurosci.* 24, 8265–8277.

Chen, L.L., Lin, L.H., Green, E.J., Barnes, C.A., and McNaughton, B.L. (1994). Head-direction cells in the rat posterior cortex. I. Anatomical distribution and behavioral modulation. *Exp. Brain Res. Exp. Hirnforsch. Expérimentation Cérébrale* *101*, 8–23.

Clark, B.J., Harris, M.J., and Taube, J.S. (2012). Control of anterodorsal thalamic head direction cells by environmental boundaries: Comparison with conflicting distal landmarks. *Hippocampus* *22*, 172–187.

Diba, K., and Buzsaki, G. (2008). Hippocampal network dynamics constrain the time lag between pyramidal cells across modified environments. *J. Neurosci.* *28*, 13448.

Ding, S.-L. (2013). Comparative anatomy of the prosubiculum, subiculum, presubiculum, postsubiculum, and parasubiculum in human, monkey, and rodent. *J. Comp. Neurol.* *521*, 4145–4162.

Doeller, C.F., King, J.A., and Burgess, N. (2008). Parallel striatal and hippocampal systems for landmarks and boundaries in spatial memory. *Proc. Natl. Acad. Sci.* *105*, 5915.

Etienne, A.S., and Jeffery, K.J. (2004). Path integration in mammals. *Hippocampus* *14*, 180–192.

Etienne, A.S., Maurer, R., Boulens, V., Levy, A., and Rowe, T. (2004). Resetting the path integrator: a basic condition for route-based navigation. *J. Exp. Biol.* *207*, 1491–1508.

Felleman, D.J., and Van Essen, D.C. (1991). Distributed Hierarchical Processing in the Primate Cerebral Cortex. *Cereb. Cortex* *1*, 1–47.

Giocomo, L.M., Stensola, T., Bonnevie, T., Van Cauter, T., Moser, M.-B., and Moser, E.I. (2014). Topography of head direction cells in medial entorhinal cortex. *Curr. Biol. CB* *24*, 252–262.

Goodridge, J.P., and Taube, J.S. (1997). Interaction between the postsubiculum and anterior thalamus in the generation of head direction cell activity. *J. Neurosci.* *17*, 9315–9330.

Gothard, K.M., Skaggs, W.E., and McNaughton, B.L. (1996). Dynamics of mismatch correction in the hippocampal ensemble code for space: interaction between path integration and environmental cues. *J. Neurosci. Off. J. Soc. Neurosci.* *16*, 8027–8040.

Hafting, T., Fyhn, M., Molden, S., Moser, M.-B., and Moser, E.I. (2005). Microstructure of a spatial map in the entorhinal cortex. *Nature* *436*, 801–806.

Hardcastle, K., Ganguli, S., and Giocomo, L.M. (2015). Environmental boundaries as an error correction mechanism for grid cells. *Neuron* *86*, 827–839.

Hargreaves, E.L., Rao, G., Lee, I., and Knierim, J.J. (2005). Major Dissociation Between Medial and Lateral Entorhinal Input to Dorsal Hippocampus. *Science* *308*, 1792–1794.

Harris, K.D. (2005). Neural signatures of cell assembly organization. *Nat. Rev. Neurosci.* *6*, 399–407.

Hinman, J.R., Brandon, M.P., Climer, J.R., Chapman, G.W., and Hasselmo, M.E. (2016). Multiple Running Speed Signals in Medial Entorhinal Cortex. *Neuron* *91*, 666–679.

Horev, G., Benjamini, Y., Sakov, A., and Golani, I. (2007). Estimating wall guidance and attraction in mouse free locomotor behavior. *Genes Brain Behav.* *6*, 30–41.

Knierim, J.J., and Zhang, K. (2012). Attractor Dynamics of Spatially Correlated Neural Activity in the Limbic System. *Annu. Rev. Neurosci.* *35*, 267–285.

Kropff, E., Carmichael, J.E., Moser, M.-B., and Moser, E.I. (2015). Speed cells in the medial entorhinal cortex. *Nature*.

Krupic, J., Burgess, N., and O'Keefe, J. (2012). Neural representations of location composed of spatially periodic bands. *Science* 337, 853–857.

Krupic, J., Bauza, M., Burton, S., Barry, C., and O'Keefe, J. (2015). Grid cell symmetry is shaped by environmental geometry. *Nature* 518, 232–235.

Langston, R.F., Ainge, J.A., Couey, J.J., Canto, C.B., Bjerknes, T.L., Witter, M.P., Moser, E.I., and Moser, M.-B. (2010). Development of the spatial representation system in the rat. *Science* 328, 1576–1580.

Leutgeb, S., Ragozzino, K.E., and Mizumori, S.J. (2000). Convergence of head direction and place information in the CA1 region of hippocampus. *Neuroscience* 100, 11–19.

Lever, C., Burton, S., Jeewajee, A., O'Keefe, J., and Burgess, N. (2009). Boundary Vector Cells in the Subiculum of the Hippocampal Formation. *J. Neurosci.* 29, 9771–9777.

McNaughton, B.L., Battaglia, F.P., Jensen, O., Moser, E.I., and Moser, M.-B. (2006). Path integration and the neural basis of the “cognitive map.” *Nat. Rev. Neurosci.* 7, 663–678.

Mittelstaedt, M.L., and Mittelstaedt, H. (1980). Homing by path integration in a mammal. *Naturwissenschaften* 67, 566–567.

Muller, R.U., and Kubie, J.L. (1987). The effects of changes in the environment on the spatial firing of hippocampal complex-spike cells. *J. Neurosci. Off. J. Soc. Neurosci.* 7, 1951–1968.

O'Keefe, J., and Burgess, N. (1996). Geometric determinants of the place fields of hippocampal neurons. *Nature* 381, 425–428.

O'Keefe, J., and Dostrovsky, J. (1971). The hippocampus as a spatial map. Preliminary evidence from unit activity in the freely-moving rat. *Brain Res.* 34, 171–175.

O'Keefe, J., and Nadel, L. (1978). *The hippocampus as a cognitive map* (Clarendon Press Oxford).

Pastalkova, E., Itskov, V., Amarasingham, A., and Buzsaki, G. (2008). Internally generated cell assembly sequences in the rat hippocampus. *Science* 321, 1322.

Peyrache, A., Lacroix, M.M., Petersen, P.C., and Buzsáki, G. (2015). Internally organized mechanisms of the head direction sense. *Nat. Neurosci.* 18, 569–575.

Preston-Ferrer, P., Coletta, S., Frey, M., and Burgalossi, A. (2016). Anatomical organization of presubicular head-direction circuits. *eLife* 5, e14592.

Ranck, J.B. (1985). Head direction cells in the deep cell layer of dorsal presubiculum in freely moving rats. In *Electrical Activity of Archicortex.*, G. Buzsáki, and Vanderwolf, C. H., eds. (Budapest: Akademiai Kiado), pp. 217–220.

Rubin, A., Yartsev, M.M., and Ulanovsky, N. (2014). Encoding of head direction by hippocampal place cells in bats. *J. Neurosci. Off. J. Soc. Neurosci.* 34, 1067–1080.

Samsonovich, A., and McNaughton, B.L. (1997). Path integration and cognitive mapping in a continuous attractor neural network model. *J. Neurosci.* 17, 5900.

Sargolini, F., Fyhn, M., Hafting, T., McNaughton, B.L., Witter, M.P., Moser, M.-B., and Moser, E.I. (2006). Conjunctive representation of position, direction, and velocity in entorhinal cortex. *Science* 312, 758–762.

Savelli, F., Yoganarasimha, D., and Knierim, J.J. (2008). Influence of boundary removal on the spatial representations of the medial entorhinal cortex. *Hippocampus* 18, 1270–1282.

Sharp, P.E. (1996). Multiple spatial/behavioral correlates for cells in the rat postsubiculum: multiple regression analysis and comparison to other hippocampal areas. *Cereb. Cortex* N. Y. N 1991 6, 238–259.

Sharp, P.E., Blair, H.T., and Cho, J. (2001). The anatomical and computational basis of the rat head-direction cell signal. *Trends Neurosci.* 24, 289–294.

Shibata, H. (1993). Direct projections from the anterior thalamic nuclei to the retrohippocampal region in the rat. *J. Comp. Neurol.* 337, 431–445.

Sofroniew, N.J., Vlasov, Y.A., Andrew Hires, S., Freeman, J., and Svoboda, K. (2015). Neural coding in barrel cortex during whisker-guided locomotion. *eLife* 4.

Solstad, T., Boccara, C.N., Kropff, E., Moser, M.-B., and Moser, E.I. (2008). Representation of Geometric Borders in the Entorhinal Cortex. *Science* 322, 1865–1868.

Stensola, T., Stensola, H., Moser, M.-B., and Moser, E.I. (2015). Shearing-induced asymmetry in entorhinal grid cells. *Nature* 518, 207–212.

Tan, H.M., Bassett, J.P., O'Keefe, J., Cacucci, F., and Wills, T.J. (2015). The development of the head direction system before eye opening in the rat. *Curr. Biol.* CB 25, 479–483.

Tang, Q., Burgalossi, A., Ebbesen, C.L., Sanguinetti-Scheck, J.I., Schmidt, H., Tukker, J.J., Naumann, R., Ray, S., Preston-Ferrer, P., Schmitz, D., et al. (2016). Functional Architecture of the Rat Parasubiculum. *J. Neurosci.* 36, 2289–2301.

Taube, J.S. (1995). Head direction cells recorded in the anterior thalamic nuclei of freely moving rats. *J. Neurosci.* 15, 70–86.

Taube, J.S. (2007). The head direction signal: origins and sensory-motor integration. *Annu. Rev. Neurosci.* 30, 181–207.

Taube, J.S., Muller, R.U., and Ranck, J.B. (1990a). Head-direction cells recorded from the postsubiculum in freely moving rats. I. Description and quantitative analysis. *J. Neurosci.* 10, 420–435.

Taube, J.S., Muller, R.U., and Ranck, J.B., Jr (1990b). Head-direction cells recorded from the postsubiculum in freely moving rats. II. Effects of environmental manipulations. *J. Neurosci.* 10, 436–447.

Truccolo, W., Eden, U.T., Fellows, M.R., Donoghue, J.P., and Brown, E.N. (2005). A point process framework for relating neural spiking activity to spiking history, neural ensemble, and extrinsic covariate effects. *J. Neurophysiol.* 93, 1074–1089.

Tukker, J.J., Tang, Q., Burgalossi, A., and Brecht, M. (2015). Head-Directional Tuning and Theta Modulation of Anatomically Identified Neurons in the Presubiculum. *J. Neurosci.* 35, 15391–15395.

Wills, T.J., Cacucci, F., Burgess, N., and O'Keefe, J. (2010). Development of the hippocampal cognitive map in preweanling rats. *Science* 328, 1573–1576.

Wilson, M.A., and McNaughton, B.L. (1993). Dynamics of the hippocampal ensemble code for space. *Science* 261, 1055–1058.

Wiltschko, A.B., Johnson, M.J., Iurilli, G., Peterson, R.E., Katon, J.M., Pashkovski, S.L., Abaira, V.E., Adams, R.P., and Datta, S.R. (2015). Mapping Sub-Second Structure in Mouse Behavior. *Neuron* 88, 1121–1135.

Winter, S.S., Clark, B.J., and Taube, J.S. (2015). Disruption of the head direction cell network impairs the parahippocampal grid cell signal. *Science* 1259591.

Zugaro, M.B., Berthoz, A., and Wiener, S.I. (2001). Background, but not foreground, spatial cues are taken as references for head direction responses by rat anterodorsal thalamus neurons. *J. Neurosci. Off. J. Soc. Neurosci.* 21, RC154.

Zugaro, M.B., Arleo, A., Berthoz, A., and Wiener, S.I. (2003). Rapid spatial reorientation and head direction cells. *J. Neurosci.* 23, 3478–3482.

Figures

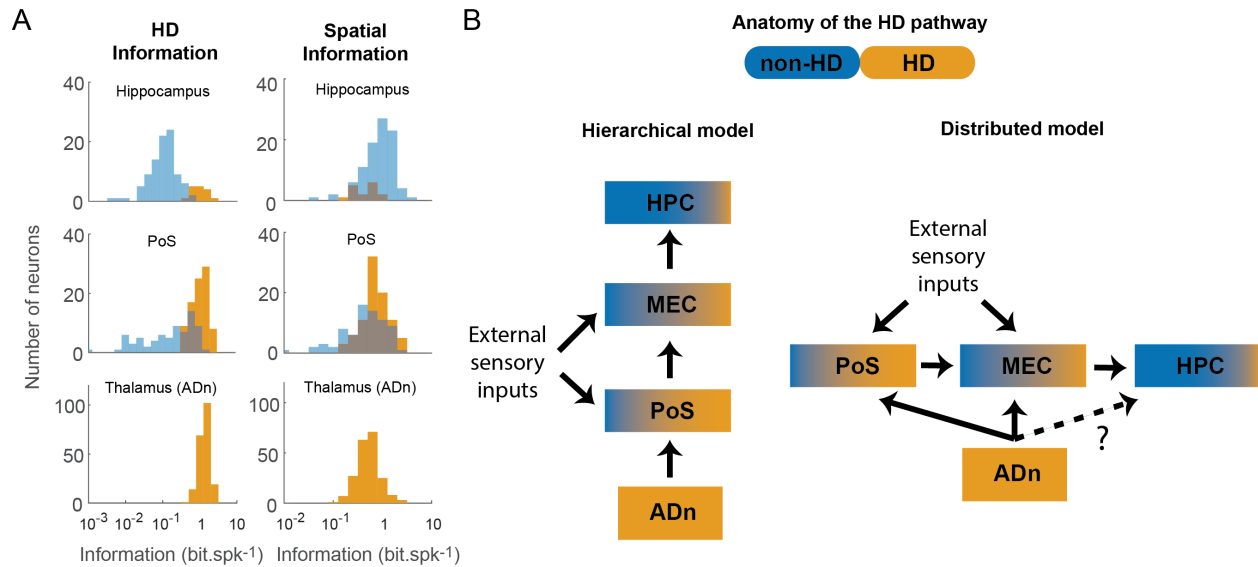


Figure 1 – Anatomical organization of neural information relevant to navigation.

(A) Distribution of head-direction (left) and spatial (right) information in the ADn, PoS and hippocampus for HD neurons (orange) and non-HD pyramidal cells (blue). (B) Schematic diagram of HD signal transformation to spatial information in a hierarchical (left) or distributed (right) fashion.

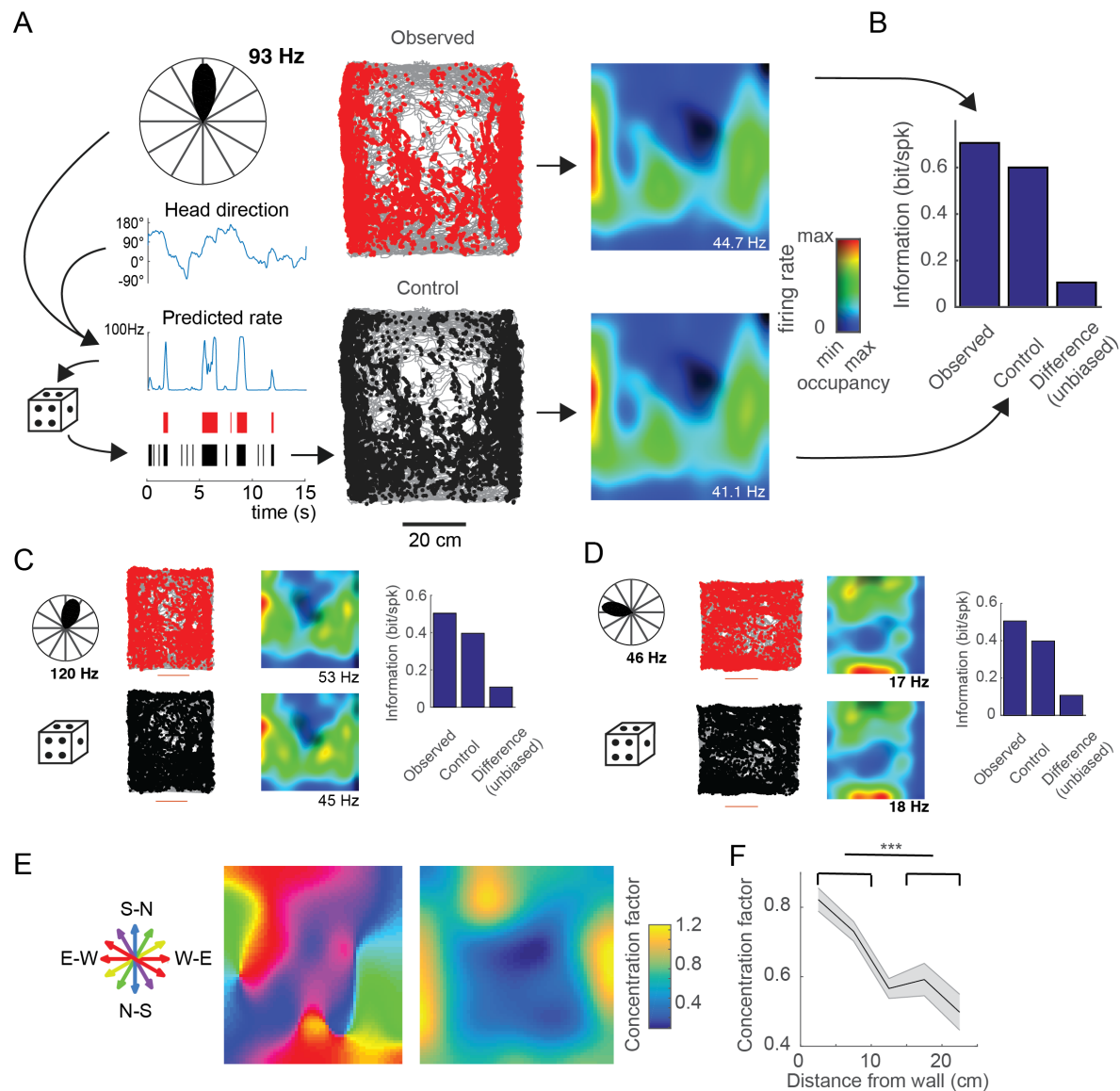


Figure 2 - HD cells convey spatial information.

(A) Example of a HD cells recorded in the ADn. Top left, HD tuning curve (average firing rate in function of animal's orientation); top middle: position of the animal (grey) superimposed with location of the animal when the neuron spiked (red dots); top right, spatial tuning of the neuron where average firing rate at each location is represented as a colormap. Contrast displays the overall occupancy at each location. Bottom, same as top panels for a random spike train generated from the HD tuning curve only.

(B) Spatial information conveyed by the neuron and by the randomly generated spike train. The difference between these two measures is referred to as ‘unbiased information’. (C-D) Two other examples of HD neurons recorded from the ADn presented as in (A-B). (E) Left, average orientation of animal’s displacement for the session shown in (A); right, concentration factor of these orientations around their mean. (F) Average (\pm s.e.m.) concentration of orientation as a function of distance to the nearest wall.

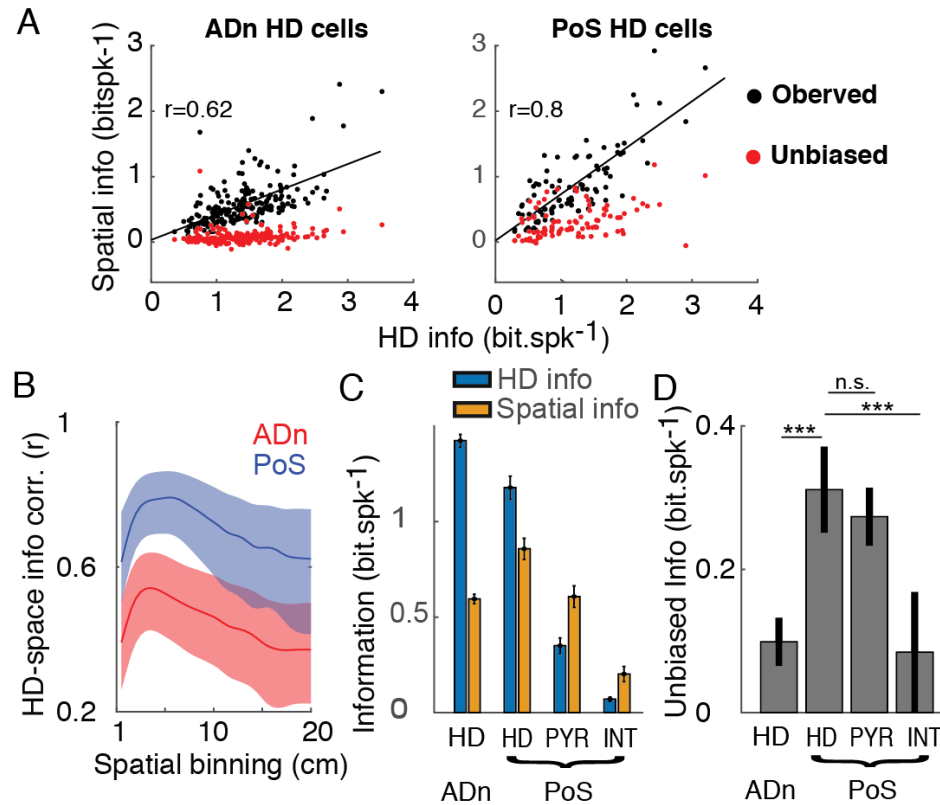


Figure 3. HD and spatial information covary.

(A) HD and spatial information of each HD neurons in the ADn (left) and the PoS (right). Lines indicate best linear fits ($p < 10^{-10}$ for ADn and PoS, Pearson's test). (B) Average (\pm s.e.m.) HD (blue) and spatial (orange) information for (from left to right) HD neurons recorded in the ADn, in the PoS, PoS putative pyramidal (PYR) and interneurons (INT). (C) Average (\pm s.e.m.) unbiased spatial information for the same categories as in b ($***p < 10^{-10}$; n.s. $p > 0.05$). (D) Correlation between HD and spatial information in function of spatial binning for PoS (blue) and ADn (red) neurons.

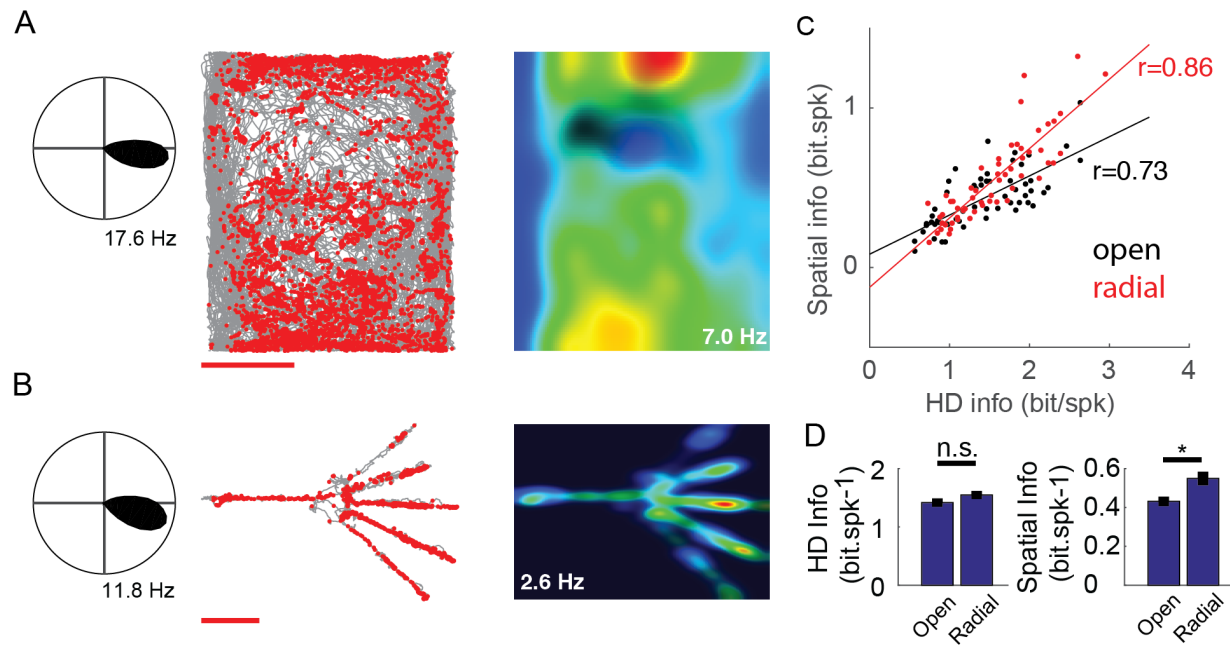


Figure 4. HD and spatial information correlation is modulated by the environmental constrain on animal's behavior.

(A) Example of a HD cell recorded in the ADn in an open environment, presented as in Figure 1. (B) The same neuron now recorded in a 6 arm maze. (C) Neuron-by-neuron correlation of HD and spatial information and linear of best linear fit ($p < 10^{-10}$ for both conditions, $n=57$, Pearson's test). (D) Average (\pm s.e.m.) HD (left) and spatial (right) information in both environments (* $p < 0.01$, sign test; n.s. $p > 0.05$)

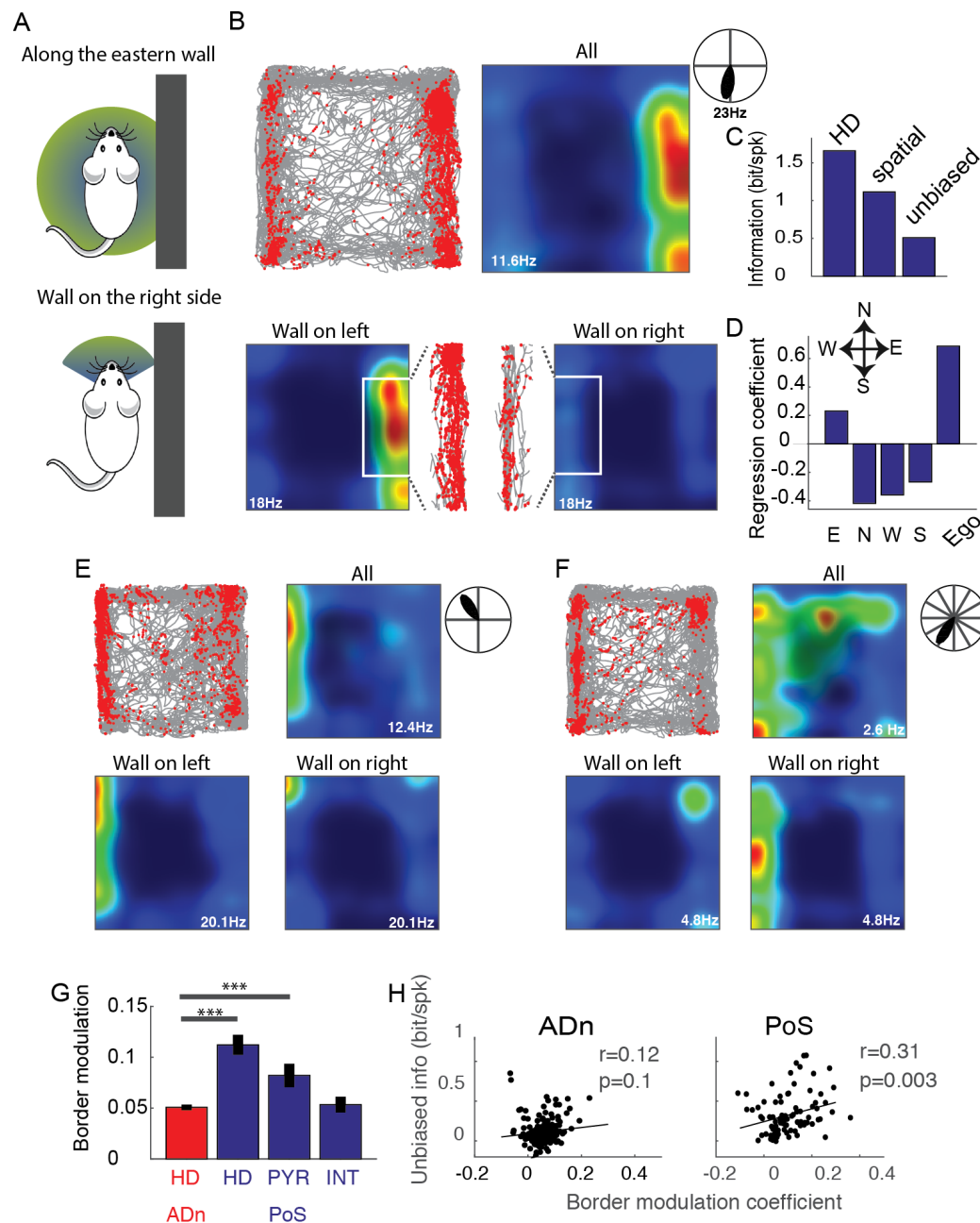


Figure 5. HD neurons integrate allocentric (vestibular) and egocentric (self-centered)

information to build an unbiased spatial code.

(A) Schemas depicting the two types of behavioral variables used to regress the neuronal data on. Top, specific border sensitivity (East, North, West or South) independently of animal's head-direction; bottom, animal's position relative to the closest wall ('all on the right' or 'wall on the

left') within a $\pm 60^\circ$ range of head direction. (B) Top, HD neuron recorded in the PoS, same presentation as in Figure 1. Bottom, place fields of the neuron during exploration along the borders when the walls are located on the left of the animal (left panel) or on the right (right panel). Inset show animal's position and spike location in the two configuration during which a neuron governed only by its HD tuning curve is expected to fire. (C) HD, spatial and unbiased information per spike of the neuron shown in a. (D) Regression coefficients of the generalized linear model applied to the binned spike train of the neuron displayed in a, consisting of walls (E-N-W-S) or relative wall position (Ego), both regression included expected instantaneous firing rate from HD tuning curve. (E) Average (\pm s.e.m.) border modulation and egocentric modulation for neuronal group. *** $p < 0.001$. (F) Unbiased spatial information in function of egocentric modulation. Texts indicate Pearson's correlations (r) and p values.

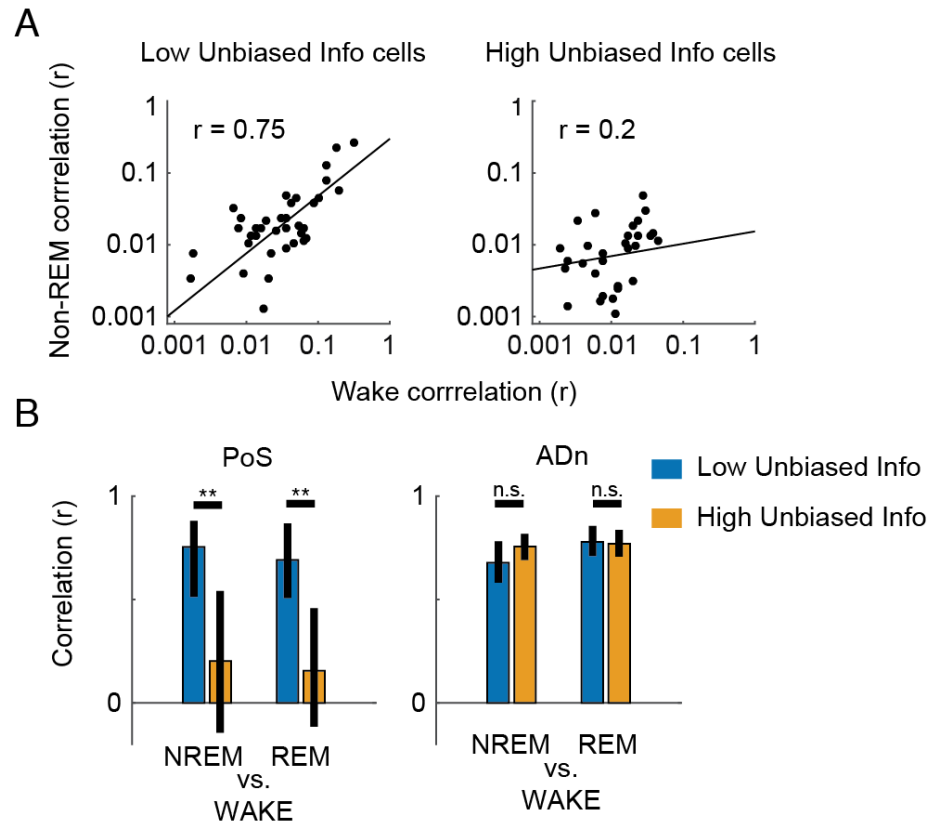


Figure 6. Functional connectivity of spatially-related cells is not rigid.

(A) left: Pairwise neuronal correlation during non-REM versus wake for PoS cell pairs with low unbiased spatial information (bottom 33% percentile); right, same for cell pairs conveying high unbiased spatial information (top 33% percentile). (B) left, cross-brain states correlations (non-REM versus wake and REM versus wake) in the PoS for neuron pairs conveying low (blue) and high (orange) unbiased spatial information; right, same for ADn cell pairs. **: $p < 0.01$; error bars indicate 95% confidence interval.

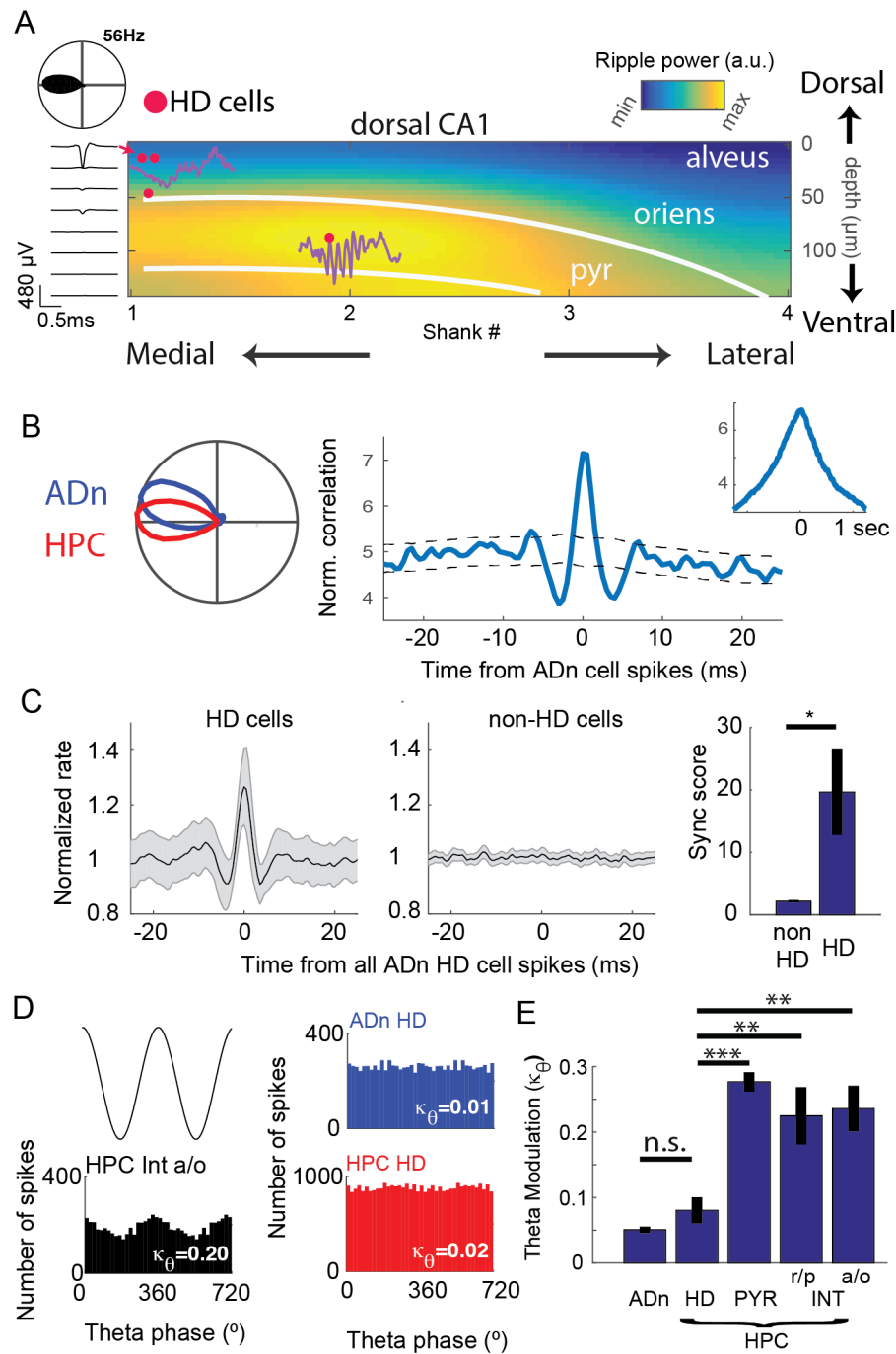
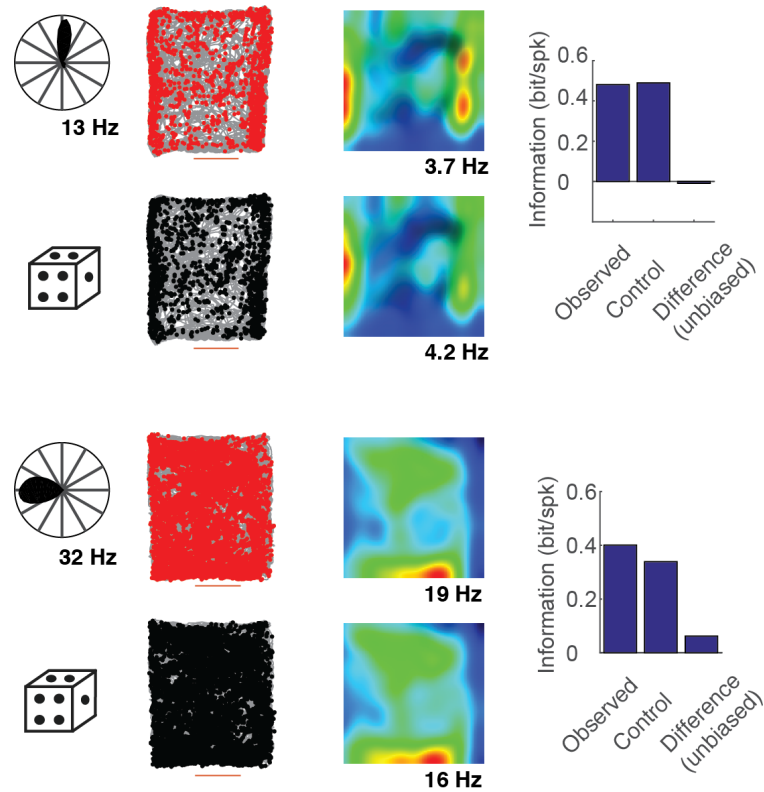


Figure 7. Direct HD signal inputs to the hippocampus / subiculum.

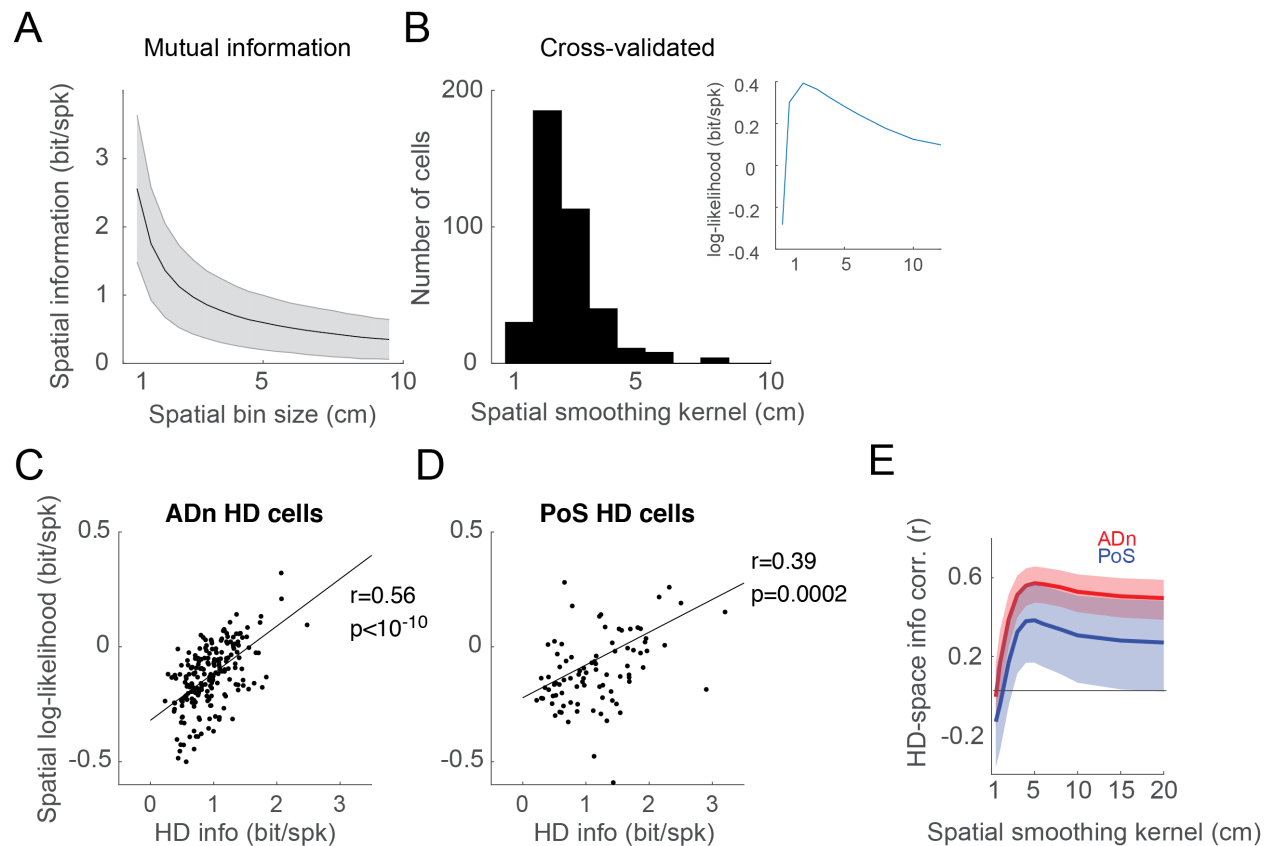
(A) Anatomical mapping of ripple power recorded with a 32 site (4 shanks x 8 sites) silicon probe. An example HD cells recorded on the most medial shank, putatively located in the oriens/alveus. (B) Two HD cells simultaneously recorded in the ADn and the hippocampus with overlapping tuning curves (left). Fine temporal cross-correlogram between the two spike trains

reveals submillisecond synchronous firing between the two units. Cross-correlogram at larger timescale shows behaviorally-induced positive correlation (inset). (C) Average cross-correlogram between individual HD (left) and non-HD (right) neurons in the hippocampus and all spikes from isolated ADn neurons. (D) Action potential phases relative to theta oscillation (6-12 Hz) during spatial exploration of three simultaneously recorded neurons: the same HD neurons from ADn (blue) and CA1 (red) shown. (E) Average (\pm s.e.m.) theta modulation (see METHODS) of ADn neurons and hippocampal neurons (PYR: non-HD pyramidal neurons; HD: hippocampal HD neurons from the alveus/oriens; INT: non-HD interneurons; r/p: radiatum/pyramidal layer; a/o: alveus/oriens layer). * $p < 0.05$, ** $p < 0.01$, *** $p < 0.001$.

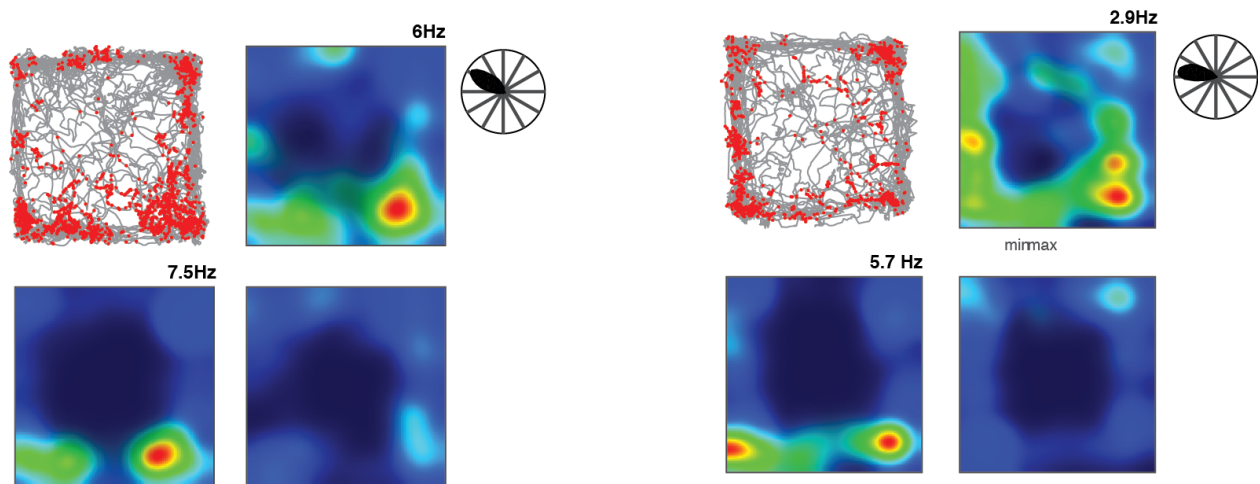
Supplementary Figures



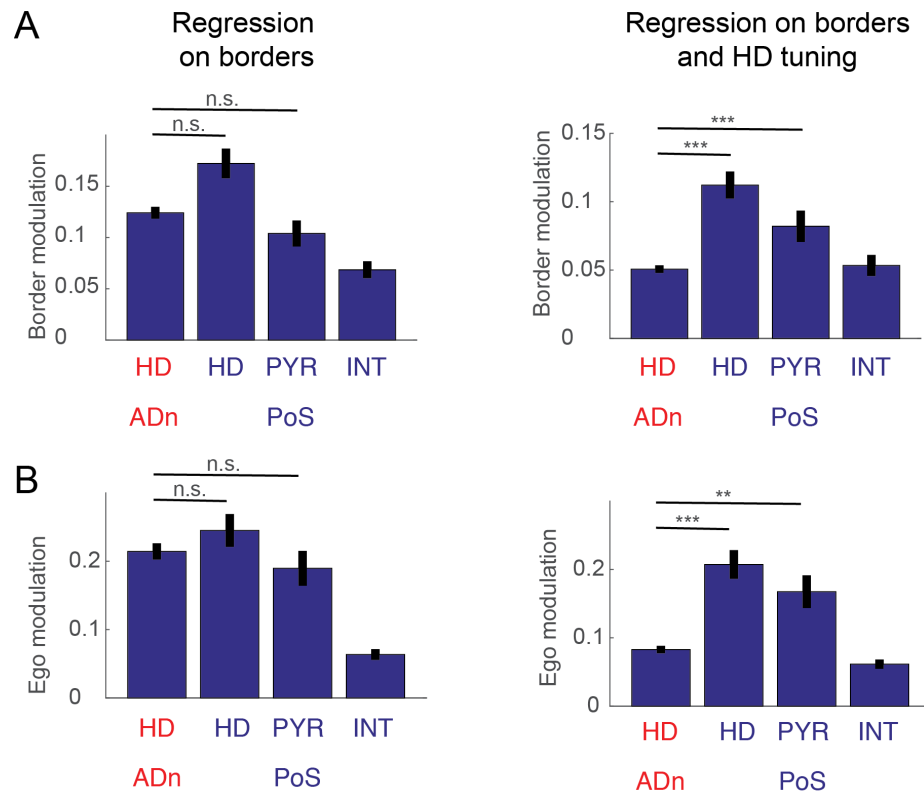
Supplementary Figure 1. Additional examples of ADn HD neurons. Same presentation as in Figure 1. Top three panels display (from left to right): HD tuning curve; trajectory (grey) and spike positions (red dots); place field (color coded, dark red: maximal firing rate; dark blue: null firing rate). Bottom two panels present data from an artificially generated spike train based on the neuron HD tuning curve and animal's position and heading. Bar plot on the right display amount of observed, control and unbiased spatial information per spike.



Supplementary Figure 2. Cross-validated spatial information measures confirm the HD-spatial information relationship. (A) Mutual information decreases with the size of spatial bins (mean \pm s.t.d.; all HD cells included;). (B) Distribution of spatial kernel widths that maximized the cross-validated spatial log-likelihood; inset displays the example of spatial log-likelihood in function of spatial smoothing width for an example neuron. (C) Spatial log-likelihood versus HD information for ADn HD neurons. d, same as c for HD neurons recorded in the PoS. (E) Correlation between spatial log-likelihood and HD information versus spatial smoothing width for ADn (red) and PoS (blue) HD neurons; shaded areas represent 95% interval of confidence.



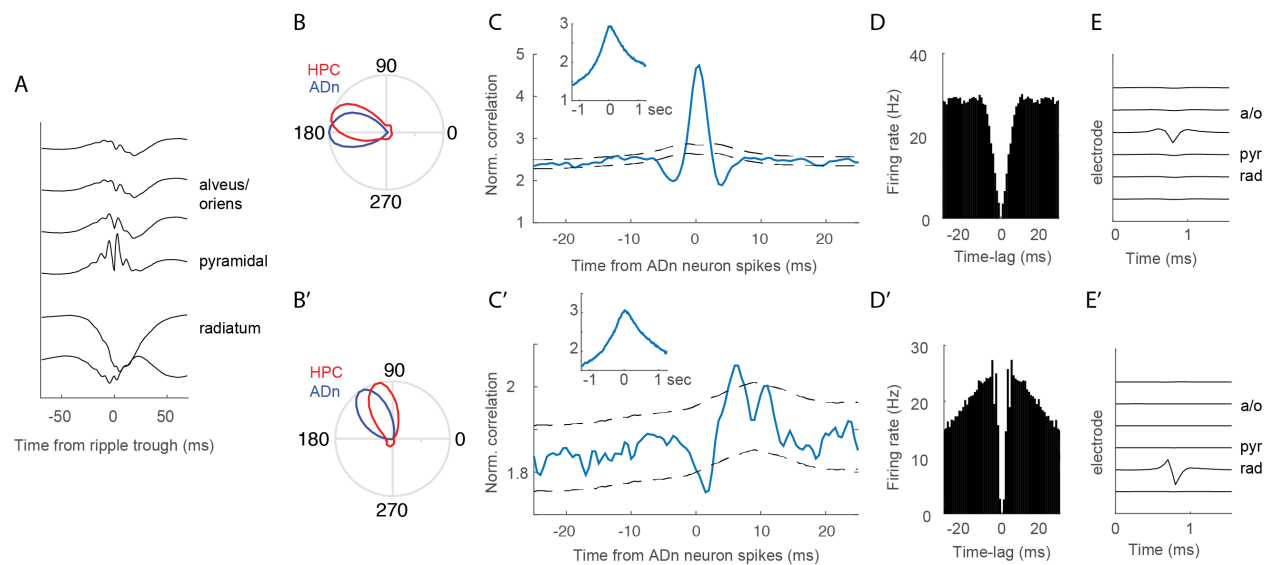
Supplementary Figure 3. Examples of PoS neurons modulated by body-wall relationship. Top panels show (from left to right) animal's trajectory and spike location (red dots), place fields and HD tuning curve. Bottom panels display place fields restricted to the 'wall on the left' (left) and 'wall on the right' (right) conditions.



Supplementary Figure 4. Regression of neuronal data with Generalized Linear Model.

(A) Binned spike trains were regressed on binary variables indicating the presence of the animals along each of the wall using a log link function (assuming neurons are Poisson processes). Left panel indicate the average (\pm s.e.m.) maximal regression coefficients (among the four coefficients associated with each wall, referred to as ‘border modulation’) for each group of neurons. The same regression was then computed by adding the expected firing rate based on animal’s behavior and HD tuning curves (right). Right panel is similar as Figure 5G.

(B) Same as (A) for regression on position of the animal relative to the walls. ‘Egocentric modulation’ was defined as the absolute difference between the regression coefficients associated with the wall on the right or the left of the animals.



Supplementary Figure 5. Two other examples of hippocampal HD neurons coordinated with the ADn, from the same recording session. (A) Ripple-triggered average (arbitrary units) of LFP recording on each of the 6 recording sites along the dorso-ventral axis of CA1. Their profile allow a precise identification of the recording layers. (B-D) An example HD neuron recorded in stratum oriens. (B) HD tuning curves of the hippocampal neuron and of a simultaneously recorded HD neuron in the ADn with an overlapping tuning. (C) Fine temporal cross-correlation reveals a near-0 synchrony with the ADn cell spike train. At larger temporal scale, the width of cross-correlation is directly related to the average time the animal spends in the overlapping section of the two HD cell's tuning curves. (D) Hippocampal cell auto-correlogram, resembling those of ADn cells (Peyrache et al., 2015). (E) Average waveform of the neuron. (B'-E') Second example HD neuron recorded in the hippocampus. This time, the cell showed a delayed spiking at fine temporal resolution with a ADn HD cell pointing toward the same direction (B'-C'), as observed between the ADn and the PoS (Peyrache et al., 2015). (D') Its auto-correlogram is narrow and is strikingly different from auto-correlograms of ADn cells.